Polymer Dynamics in Rubbery Epoxy Networks/ Polyhedral Oligomeric Silsesquioxanes Nanocomposites

Th. Kourkoutsaki,[1] E. Logakis,[1] I. Kroutilova,[2] L. Matejka,[2] J. Nedbal,[3] P. Pissis[1]

[1]*Department of Physics, National Technical University of Athens, Athens 15780, Greece*
[2]*Institute of Maromolecular Chemistry, Academy of the Sciences of the Czech Republic, 16206 Prague 6, Czech Republic*
[3]*Faculty of Mathematics and Physics, Charles University, 18000 Prague 8, Czech Republic*

Received 13 November 2008; accepted 9 February 2009
DOI 10.1002/app.30225
Published online 28 April 2009 in Wiley InterScience (www.interscience.wiley.com).

ABSTRACT: Dielectric techniques, including thermally stimulated depolarization currents (TSDC, −150 to 30°C) and, mainly, broadband dielectric relaxation spectroscopy (DRS, 10^{-2} – 10^{6} Hz, −150 to 150°C) were employed, next to differential scanning calorimetry (DSC), to investigate molecular dynamics in rubbery epoxy networks prepared from diglycidyl ether of Bisphenol A (DGEBA) and poly (oxypropylene)diamine (Jeffamine D2000, molecular mass 2000) and modified with polyhedral oligomeric silsesquioxanes (POSS) units covalently bound to the chains as dangling blocks. Four relaxations were detected and analyzed: in the order of increasing temperature at constant frequency, two local, secondary γ and β relaxations in the glassy state, the segmental α relaxation associated with the glass transition and the normal mode relaxation, related with the presence of a dipole moment component along the Jeffamine chain contour. Measurements on pure Jeffamine D2000 helped to clarify the molecular origin of the relaxations observed. A significant reduction of the magnitude and a slight acceleration of the α and of the normal mode relaxations were observed in the modified networks. These results suggest that a fraction of polymer is immobilized, probably at interfaces with POSS, due to constraints imposed by the covalently bound rigid nanoparticles, whereas the rest exhibits a slightly faster dynamics due to increaseof free volume resulting from loosened molecular packing of the chains (plasticization by the bulky POSS units).The increase of free volume is rationalized by density measurements. J Appl Polym Sci 113: 2569–2582, 2009

Key words: nanocomposites; dielectric properties; rubbery epoxy networks; polyhedral oligomeric silsesquioxanes (POSS); segmental dynamics

INTRODUCTION

Polyhedral oligomeric silsesquioxane (POSS)—polymer nanocomposites have attracted much interest as high-performance materials over the last 15 years. Earlier work has been reviewed by Pittman et al.,[1] whereas more recent advances have been summarized by Phillips et al.,[2] with particular emphasis on structure–property relationships and space-survivability testing, and by Pielichowski et al.[3]

POSS are cluster-like oligomers of the type $(R\text{-}SiO_{1.5})_n$, consisting of a silica cage with organic R groups on the corners (Scheme 1). The most common POSS compounds are those with $n = 8$, octasilsesquioxanes (T8-POSS). The POSS molecule is an ideal building block for synthesis of new organic–inorganic polymers, this building-block capability being a key benefit of POSS nanostructured chemicals.[2–8] Depending on the number of functional R groups, polymer nanocomposites with various topological localization of POSS (unbound or covalently bound as a pendant unit, as a compact block in the backbone, or as a polyhedral network junction) can be prepared.[9] The incorporation of POSS in various polymers resulted in improvement of properties, such as mechanical properties, thermal stability, flammability, gas permeability, and dielectric permittivity.[1–3]

The structure/morphology and the properties of the POSS-polymer nanocomposites were found to depend on the degree of bonding and on concentration of the POSS units. Although POSS–POSS interactions dominate in physical POSS-polymer blends and give rise to aggregation and crystallization of POSS molecules, POSS-polymer interactions become more important when the POSS units are covalently

Correspondence to: P. Pissis (ppissis@central.ntua.gr).
Contract grant sponsor: European Social Fund, Greek National Resources (25%) – (EPEAEK II) – PYTHAGORAS II.
Contract grant sponsor: Leukippus Program of the National Technical University of Athens and by the Ministry of Education of the Czech Republic; contract grant number: project MSM 0021620835.

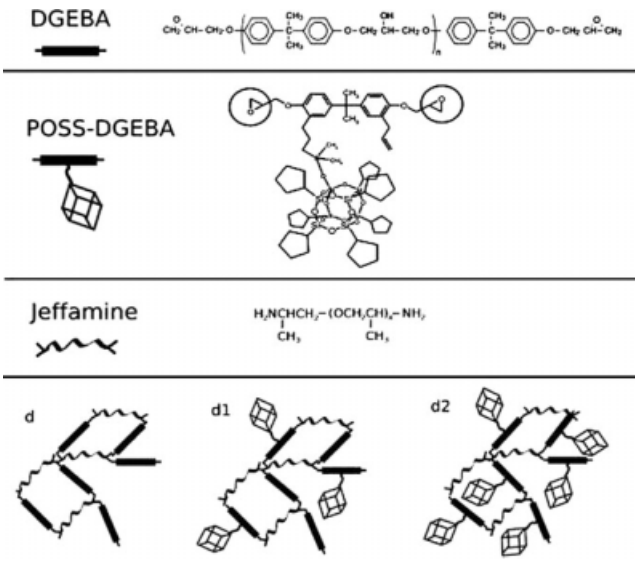

Scheme 1 Chemicals used and structure of the materials studied. See Table I for composition of the samples.

bound to the polymer chains.[10] However, even in that case, POSS–POSS interactions control to a large extent the physical properties of the modified polymers.[11]

Effects of POSS on chain mobility and relaxation have been studied mainly in terms of modification of glass transition temperature T_g. Untethered POSS has plasticizing effect and decreases T_g.[12] However, at higher POSS contents, T_g increases due to POSS-chain and POSS–POSS interactions.[13] Theoretical simulations show that aggregation of POSS moieties is not required for slowing polymer chain relaxation.[14] Toepfer et al. observed an increase of T_g in PMMA-POSS hybrids.[15] Kopesky et al. analyzed viscosity data in PMMA-POSS, tethered and untethered, and found a significant slowing down of chain relaxation in the first case and a decrease of viscosity, correlated with an increase of free volume, in the second case.[16]

Epoxy networks modified by POSS were prepared (often by using multifunctional epoxy-POSS monomers[5,8]) and investigated by several researchers. T_g was found to increase,[17] to decrease,[18] or practically not to change[19] in the modified networks, as compared with the pure epoxy network. An increase of T_g and slowing down of the chain relaxation in the glassy state was observed in epoxy networks by attachment of the monofunctional epoxy-POSS.[20] It has been pointed out that in nanocomposites with a thermosetting matrix, the presence of nanoparticles may have an effect on the curing process itself and, through that, on polymer dynamics and glass transition.[21] Special attention have attracted in recent years hybrid polymer-POSS networks with various low-dielectric permittivity polymers, such as polyimide[22,23] and poly(ε-caprolactone)[24], for preparing low-dielectric permittivity (low-κ) materials for application in microelectronics as intermetal and interlayer dielectrics. Reduction of dielectric permittivity in the hybrid networks was explained in terms of porosity and increased free volume, as indicated by a concomitant decrease in density.[22,23]

Matejka et al. reported on structure/morphology[9] and on thermomechanical properties[25] of rubbery epoxy networks reinforced with POSS incorporated as junctions in the network or bonded as dangling blocks of the network chain. WAXS, SAXS, and TEM measurements indicated that the structure of the networks is governed mainly by POSS–POSS interactions within the polymer matrix and that the pendant POSS aggregate and even crystallize in the network.[9] The POSS–POSS interaction was found to be crucial also for mechanical properties of the hybrids. It was observed that only a very high POSS content resulted in some immobilization of network chains, so that, besides a broadening of the glass transition, T_g was not practically affected.[25]

In the present article, we investigate molecular dynamics in rubbery epoxy networks with dangling POSS blocks. The hybrids were prepared and investigated with respect to structure/morphology and thermomechanical properties by Matejka and coworkers.[9,25] The rubbery epoxy network matrix was prepared from diglycidyl ether of Bisphenol A (DGEBA) and poly(oxypropylene)diamine (Jeffamine D2000, molecular mass 2000). Because of the flexibility of Jeffamine D2000, the network is characterized by low, subzero glass transition temperature T_g[9,25]. Please note that Jeffamine D2000 has been used also by Shan et al.[26] for the formation of rubbery epoxy polymers (together with diglycidyl ether of bisphenol A (Epon 828), $T_g = -38°C$ at stoichiometry), as well as for the formation of rubbery epoxy/silica nanocomposites.[27] Here, we employ broadband dielectric relaxation spectroscopy (DRS), thermally stimulated depolarization currents (TSDC) techniques, and differential scanning calorimetry (DSC) to study in detail effects of POSS on polymer dynamics. The results are discussed in terms of two contradictory effects of covalently bound inorganic inclusions on chain mobility: increase of free volume due to loosened molecular packing of the chains and constraints imposed to the motion by the rigid inclusions.[28] Detailed analysis of the time scale and of the relaxation strength (intensity, magnitude) of the dielectric relaxations present in the glassy and in the rubbery state allows to distinguish between these effects. The results obtained for polymer dynamics are correlated with those of structural/morphological characterization.[25] In addition, analysis of the temperature and the frequency dependence of dielectric permittivity may provide new insight into the origin of permittivity reduction in hybrid

polymer-POSS networks, significant with respect to design and preparation of new dielectric materials with reduced dielectric permittivity for microelectronics applications.[29]

EXPERIMENTAL

Materials

The preparation of rubbery epoxy networks modified with POSS units of various architectures (POSS units as dangling blocks, in backbone or in junction and unbound) has been described in Ref. 9. In the present work two of these hybrid nanocomposites were studied in detail, both with POSS units attached to the backbone as dangling blocks (samples d_1 and d_2 in Scheme 1 and in Table I). The reference network (sample d) was prepared from poly(oxypropylene)diamine (Jeffamine D2000, molar mass 2000 (Huntsman Inc.)) and DGEBA (SYNPO a. s. Pardubice, Czech Republic) with a stoichiometric ratio of functional groups, $r = (\mathrm{NH/epoxy}) = 1$. For the preparation of the hybrids, the DGEBA-based POSS monomer with cyclopentyl substituents, $\mathrm{POSS_{cp\text{-}DGEBA}}$ (Scheme 1) from Hybrid Plastics (Fountain Valley, CA) was used. The amount of pendant POSS was varied by varying the ratio x of the epoxy monomers, $\mathrm{POSS_{cp\text{-}DGEBA}}$, and DGEBA in the network DGEBA- $\mathrm{POSS_{cp\text{-}DGEBA}}$ (x)-D2000, keeping a constant cross-linking density ($r = 1$). The content of POSS in the networks is characterized by the weight fraction of the POSS units, $w_{\mathrm{POSS}} = m_{\mathrm{POSSunit}}/(m_{\mathrm{POSSunit}} + m_{\mathrm{DGEBA}} + m_{\mathrm{D2000}})$, where m_{DGEBA} and m_{D2000} are corresponding masses and m_{POSSunit} includes silsesquioxane cage and organic substituents except DGEBA. The weight fractions of the POSS monomers including DGEBA part are 0, 0.48, and 0.68 for samples d, d_1, and d_2, respectively. Included in Table I is also the weight fraction of cagelike Si—O skeleton without organic ligands.

Matejka et al.[9] employed WAXS, SAXS, and TEM measurements to study the structure and architecture of the hybrids under investigation there. The POSS monomer used is crystalline and the WAXS measurements showed that the POSS crystallinity is preserved in the networks. SAXS measurements performed *in situ* to follow the evolution of structure during the network formation showed that the crystal structure and the size of the crystallites are preserved. The results showed also a gradual ordering in the networks, namely a regular arrangement of POSS-crystal domains separated by extended D2000 chains. The structure model proposed on the basis of these results, involving a lamellar structure with POSS crystallinity layers, was confirmed by TEM measurements.[9] The dielectric results in this work will provide additional support for the extension of Jeffamine chains in the networks.

TABLE I
Composition of the Materials Studied

Sample	Composition	POSS (wt %)	Si—O skeleton (wt %)	Jeffamine (wt %)
d	DGEBA-D2000	0	0	85.0
d1	$\mathrm{DGEBA\text{-}POSS_{cp\text{-}DGEBA}}$ -D2000	35	15	55.0
d2	$\mathrm{POSS_{cp\text{-}DGEBA}}$-D2000	50	21	42.5

Methods

DSC measurements were carried out in the temperature range from −120 to 170°C using a Perkin-Elmer Pyris-6 calorimeter. A cooling and heating rate of 10°C/min was used.

TSDC is a dielectric technique in the temperature domain extensively used to study relaxation mechanisms in polymeric materials.[30] By this technique the sample is inserted between the plates of a capacitor and polarized by the application of an electric field E_p at temperature T_p for time t_p, which is large compared with the relaxation time of the dielectric relaxation under investigation. With the electric field still applied, the sample is cooled to a temperature T_0, which is sufficiently low to prevent depolarization by thermal energy, and then is short-circuited and reheated at a constant rate b. The discharge current generated during heating is measured as a function of temperature with a sensitive electrometer. TSDC corresponds to measuring dielectric loss at a constant low frequency in the range 10^{-4}–10^{-2} Hz. It is characterized by high sensitivity and high resolving power.[30] TSDC measurements were carried out using a Keithley 617 electrometer in combination with a Novocontrol sample cell for TSDC measurements. Typical experimental conditions were 20°C for T_p, 2 kV/cm for E_p, 5 min for t_p, 10°C/min for the cooling rate to $T_0 = -150$°C, and 3°C/min for the heating rate b.

DRS[31,32] measurements were carried out in the frequency range 10^{-2}–10^{6} Hz and the temperature range −150 to 150°C by means of a Novocontrol Alpha analyzer. The temperature was controlled to better than 0.1°C with a Novocontrol Quatro system.

For DRS and TSDC measurements the epoxy network samples, in the form of cylindrical sheets with a diameter of 20 mm and a thickness of about 0.5 mm, were placed between circular brass electrodes. For comparison pure Jeffamine D2000 was also measured by DRS and TSDC. For these measurements the liquid sample was introduced between

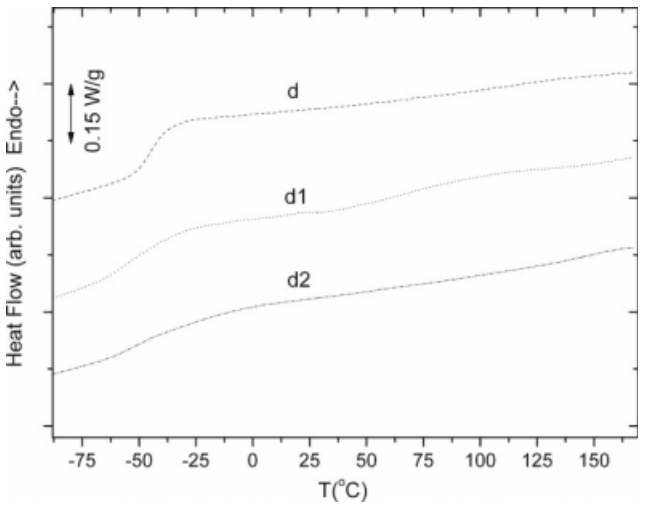

Figure 1 DSC thermograms (shifted vertically to each other, for clarity) obtained with the samples indicated on the plot. See Table I for composition of the samples.

the capacitor plates and their distance was fixed to 50 μm by means of silica spacers.

RESULTS AND DISCUSSION

DSC and TSDC measurements

DSC thermograms (second runs to delete any effects of thermal history) are shown in Figure 1, whereas the results are listed in Table II: glass transition temperature, T_g, determined as the temperature of half heat capacity increase, range of the glass transition, ΔT, determined as the difference between the temperature of completion and the temperature of onset of the glass transition, heat capacity jump at T_g, ΔC_p, and heat capacity jump normalized to the same polymer fraction in the hybrids, ΔC_{pn}, determined by $\Delta C_{pn} = \Delta C_p/(1-w)$, where w the weight fraction of the POSS unit (Table I).

T_g is in the range of about −45°C. T_g values in the same range were reported also for other epoxy networks using the flexible Jeffamine D2000 as cross-linker. T_g shows no systematic variation with composition within experimental error (±2°C), however a significant and systematic broadening with increasing weight fraction of POSS is observed. Both these results are in agreement with results reported for the same samples in reference.[25] Also, the normalized heat capacity jump at T_g, ΔC_{pn} is within experimental error (± 10%), approximately the same for the three samples studied. Please note that, although T_g, determined as the temperature of half heat capacity increase, shows no systematic variation with composition, the temperature of the onset of the transition decreases in hybrids as compared with the pure network (Fig. 1). We will comment on the significance of these results later in relation to the results obtained by TSDC and DRS.

Figure 2 shows comparative TSDC thermograms of the three samples in the temperature range from −150°C to room temperature. For comparison, the inset to Figure 2 shows the TSDC thermogram for pure Jeffamine D2000. At low temperatures, in the glassy state, a weak and broad peak, corresponding to a secondary relaxation, is observed at about −120°C. In the linear presentation and the scale of Figure 2 the peak is observed only for the pure epoxy network and Jeffamine D2000, however in a log presentation (not shown here) it is clearly observed also for the two hybrids. Secondary relaxations will be studied in more detail by DRS. At about −50°C a peak is observed in all three network samples. This peak corresponds to the segmental α relaxation associated with the glass transition. It is well established that, because of the similar range of the equivalent frequency of TSDC and of DSC measurements of about 10^{-2}–10^{-4} Hz,[30,33] the TSDC α peak is in the temperature region of calorimetric T_g.[34] For pure Jeffamine D2000 the TSDC α peak is at about −75°C (inset to Fig. 2), in agreement with the results of DSC measurements (not shown here).

The TSDC α peak in Figure 2 was analyzed in terms of peak temperature, T_a, half-width, $\Delta T_{1/2}$, and relaxation strength Δε (Table II). T_a, the temperature of current maximum, is a good measure of the calorimetric T_g.[30,34] $\Delta T_{1/2}$ is the difference between the two temperatures where the depolarization current becomes half of the current maximum. It provides a measure for the distribution of relaxation times contributing to the TSDC peak. Finally, Δε is determined by[30]

TABLE II
TSDC, DSC, and DMA Results for the α Loss Peak and the Glass Transition (Details in Text)

	DSC				TSDC			DMA	
Sample	T_g (°C)	ΔT (°C)	ΔC_p (J/g °C)	ΔC_{pn} (J/g °C)	T_α (°C)	$\Delta T_{1/2}$	$\Delta\varepsilon_n$ (°C)	T_{max}, G″ (°C)	T_{max}, tan δ (°C)
d	−44	25	0.75	0.75	−47	16	4.8	−38	−29
d1	−48	42	0.54	0.83	−50	21	1.4	−40	−24
d2	−43	70	0.36	0.72	−54	24	1.6	−48	−27

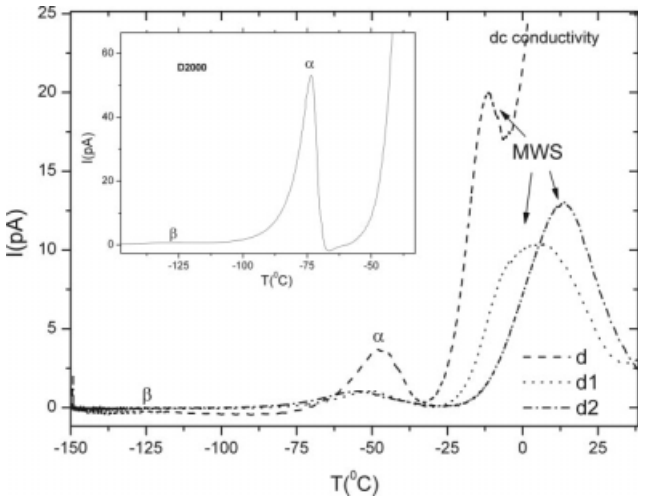

Figure 2 TSDC thermograms obtained with the samples indicated on the plot, polarized at 20°C. See Table I for composition of the samples. The inset shows the corresponding thermogram for Jeffamine D2000.

$$\Delta\varepsilon = \frac{Q}{A \cdot \varepsilon_0 \cdot E_p} \quad (1)$$

where Q the depolarization charge, determined from the area under the peak, A the surface area of the sample, E_p the polarizing field, and ε_0 the vacuum permittivity. $\Delta\varepsilon$ provides a measure for the number of relaxing units contributing to the peak. In order to compare samples with different compositions, $\Delta\varepsilon$ in Table II has been normalized to the same polymer fraction, $\Delta\varepsilon_n = \Delta\varepsilon/(1 - w)$. T_a in Table II decreases slightly but systematically with increasing POSS content, in disagreement with the DSC results. In agreement with the DSC results, a systematic broadening of the peak with increasing POSS content is observed. Finally, $\Delta\varepsilon$ is significantly reduced in the two hybrids, indicating a significant reduction of the number of relaxing units contributing to the peak.

Thus, the TSDC and the DSC results show, in agreement with each other, as well as with dynamic mechanical analysis (DMA) results for the same samples in Ref. 25, a broadening of the dielectric, thermal and mechanical response in the hybrids, with increasing POSS content, in the region of the glass transition. These results suggest increasing of heterogeneity of chain dynamics at glass transition, i. e. chain dynamics is different in different regions of the sample. The characteristic size of these regions must be larger than the characteristic length (cooperativity length) of the glass transition, which has been determined for various polymers to be in the range 1–4 nm.[35] The spatial heterogeneity in the hybrids can be understood in terms of the two main effects caused by the presence and the covalent bonding of the POSS units[28]: increase of free volume due to loosened molecular packing of the chains and constraints imposed to the motion of the chains by the rigid particles.

The TSDC results for the α relaxation show that the relaxation becomes slightly but systematically faster (i. e. T_g decreases) with increasing POSS content, whereas the normalized magnitude (relaxation strength) decreases. Interestingly, evaluation of the DMA data reported in Ref. 25 for the same samples in terms of loss modulus, instead of tan δ , shows that T_g systematically decreases in the hybrids (Table II) with a concomitant decrease of the loss peak. Please note also that a decrease of T_g in the hybrids as compared with the pure network is obtained by DSC, if the onset of the transition instead of the temperature of the half heat capacity increase is considered as T_g (Fig. 1). It should be mentioned here that the DRS results, to be reported later, reveal the existence of a second, slower, and weaker relaxation in the temperature region of the glass transition, the so-called normal mode relaxation, to be studied in detail by DRS. However, the conclusions drawn from the TSDC results on the time scale and the magnitude of the α relaxation remain valid. The acceleration of the α relaxation can be understood as a result of increase of free volume, whereas the reduction of the relaxation strength indicates that a fraction of the chains is immobilized due to constraints imposed by the presence and the covalent bonding of the POSS units.

In order to check the hypothesis about increase of free volume in the hybrids, the specific mass of the three network samples under investigation was measured, by measuring the surface area and the thickness of the samples and by weighing. The experimental values obtained were $\rho = 0.95$, 1.02, and 1.05 g/cm^3 for samples d, d_1, and d_2, respectively (experimental error ± 0.01 g/cm^3). The experimental values for the hybrids were compared with the theoretical ones calculated by additivity from the specific mass values of the pure network (sample d) and of POSSCP-DGEBA (1.20 g/cm^3), $\rho_{th} = 1.04$ and 1.075 g/cm^3 for samples d_1 and d_2, respectively. Thus, density decreases in both hybrids, as compared with the theoretical one calculated on the basis of additivity, i.e. free volume increases in the hybrids, although changes are small, close to experimental error. Similar results were obtained with polyimide-POSS hybrid nanocomposites with covalent bonds between the two components.[22,23] In poly(bisphenol A carbonate)-POSS nanocomposites prepared by solution blending, on the other hand, without chemical bonds between the two components, the experimental density was found to decrease, as compared with the theoretical one, at low POSS contents, and to become equal to the latter at higher POSS contents when phase separation occurs.[36]

Thus, a two-phase model of polymer dynamics in the hybrids can be postulated on the basis of the TSDC results, in agreement also with the DMA results: a fraction of the chains is immobilized, due to constraints imposed by tethering to the POSS nanoparticles, whereas the rest is characterized by a slightly faster dynamics. We will come back to these results later and provide further support for this two-phase model, in particular by DRS measurements. It is interesting to note, however, that the dielectric (DRS and TSDC) results are not confirmed by the DSC results, which are less conclusive with respect to effects of POSS on T_g and ΔC_p. This situation is often encountered in chain dynamics studies in polymeric systems and is sometimes explained in terms of the different nature of DSC (static), on the one hand, and dielectric and DMA (dynamic) techniques, on the other hand.[37–39] In a recent study on DSC in polymer nanocomposites attention was drawn to the difficulties of unambiguously determining the heat capacity jump ΔC_p at the glass transition (and, thus, the fraction of immobilized polymer).[40]

At temperatures higher than T_g, in the rubbery state, a strong TSDC peak is observed in the pure epoxy network at about −10°C, followed by steep increase of the depolarization current. The large magnitude of the peak indicates that its origin cannot be dipolar. In agreement with results obtained with other epoxy networks,[41] the peak is attributed to interfacial Maxwell-Wagner-Sillars (MWS) relaxation. Such a peak is characteristic for heterogeneous samples and arises from the accumulation of charges at interfaces separating regions of different electrical conductivity.[30] The steep increase of depolarization current at temperatures higher than about −10°C in the pure epoxy networks arises from dc conductivity. In the hybrids, the interfacial MWS peak is shifted to higher temperatures, becomes broader and its magnitude is reduced. These results indicate a change in the heterogeneity of the hybrids, obviously arising from the presence of the POSS units, which will not be further analyzed and quantified in the present study. It is interesting to note, however, that the shift of the MWS peak to higher temperatures in the hybrids, corresponding to larger relaxation times in isothermal measurements, is consistent with the findings of a recent NMR study on the same materials showing an increase of the size of heterogeneities (domains and aggregates) from 0.6 to 0.7 nm in the pure epoxy network to several nanometer in the hybrids.[42] Interfacial polarization was recently studied by DRS in poly(bisphenol A carbonate)-POSS nanocomposites and the relaxation was found to become slower with increasing POSS content, as the size of the conductive POSS-rich islands increases.[36] Finally, the steep increase of the depolarization current, following the MWS peak in the pure epoxy network, is not observed in the hybrids, indicating reduced dc conductivity in the hybrids, as compared with the pure epoxy networks, in agreement with DRS results to be reported in what follows.

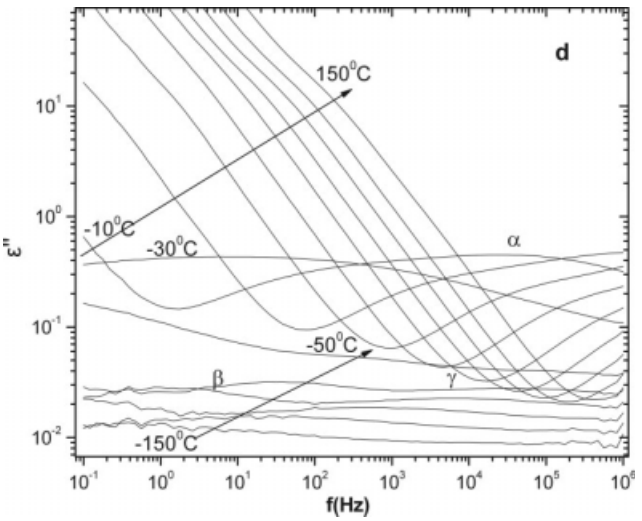

Figure 3 Frequency dependence of the imaginary part of dielectric permittivity, ε″(*f*), for the pure epoxy network (sample d) at temperatures between −150 and 150°C in steps of 20°C.

DRS measurements

Figure 3 shows results for the frequency dependence of the imaginary part of dielectric permittivity, ε″(*f*), in the pure epoxy network, over wide ranges of temperature, from −150 to 150°C, in a log–log plot. The broad frequency and temperature ranges allow to follow all the relaxations present in the samples, dipolar relaxations at lower temperatures/higher frequencies, and relaxations related with charge carrier motion at higher temperatures/lower frequencies, as steps in ε′(*f*) (not shown here) and, more clearly, as peaks in ε″(*f*). Measurements were performed in steps of 5 or 10°C, for clarity only a few of them in steps of 20°C are shown in Figure 3. Starting with low temperatures a weak peak is discerned, located at about 1 kHz at −110°C, in the following designated as γ loss peak (relaxation). The peak shifts to higher frequencies with increasing temperature, whereas a second peak enters into the frequency window of measurements, located in the range 1–10 Hz at −80°C and designated in the following as β loss peak. At higher temperatures, close to and above T_g, a broad loss peak, by one order of magnitude stronger than the secondary γ and β loss peaks, enters into the frequency window of measurements, located at about 10–100 kHz at −10°C, the α loss peak associated with the glass transition

(dynamic glass transition[35]). The peak shifts rapidly to higher frequencies with increasing temperature and a shoulder on the low-frequency side of the α peak becomes visible, located at about 100 Hz at −10°C. This shoulder is due to the normal mode (NM) relaxation, characteristic of polymers having a dipole moment component along the chain contour and related with the fluctuation and orientation of the end-to-end polarization vector of the chain.[43,44] Jeffamine has a dipole moment component aligned parallel to the chain contour and, thus, exhibits, in addition to the segmental α relaxation, associated with the glass transition, the slower NM relaxation.[45] The NM relaxation is active also in the networks, where the Jeffamine chains are covalently bonded at both ends, since the Jeffamine chains are dipole-inverted, i.e. the dipole moments of the segments are inverted in the middle of the chain.[43,44,46] Comparison with DRS spectra recorded on pure Jeffamine D2000 in the following plots will confirm that all four relaxations (γ, β, α, NM in the order of decreasing frequency/increasing temperature) in the pure rubbery epoxy network and the hybrids originate from or become dielectically active through Jeffamine D2000. At higher temperatures and lower frequencies ε″ in Figure 3 exhibit high values related with charge carrier (ion) motion and space charge polarization,[31] in agreement with the TSDC results in Figure 2.

The hybrids d_1 and d_2 exhibit dielectric spectra similar to those shown for the pure epoxy network in Figure 3. Figures 4 and 5 show comparative isochronal (constant frequency) ε′(*T*) and ε″(*T*) plots, respectively, which give an overview of the overall dielectric behavior of the materials under investigation. The data have been recorded isothermally and replotted here. A high frequency, 680 kHz, has been

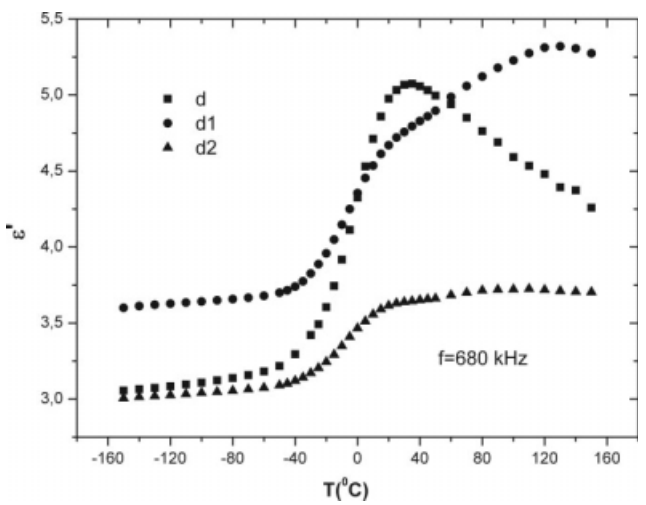

Figure 4 Comparative isochronal ε′(*T*) plot of the three networks at 680 kHz.

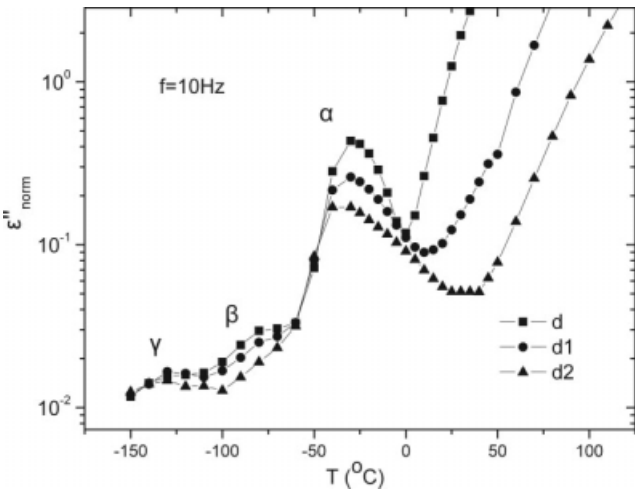

Figure 5 Comparative isochronal $\varepsilon''_{norm}(T)$ plot of the three networks at 10 Hz.

chosen for the ε′(*T*) plot to get rid of space charge polarization and other conductivity effects[47] and follow the bulk dielectric behavior of the samples under investigation.

The step in the temperature range of −60 to 25°C in ε′(*T*) in Figure 4 is related with the segmental α relaxation and the NM relaxation, which, at the high frequency of measurements, are frozen at lower temperatures and unfreeze at higher temperatures. The step is larger for sample d and becomes smaller with increasing POSS fraction in the hybrids. For the pure epoxy network ε′(*T*) decreases with increasing temperature at temperatures higher than about 25°C, as typically observed in amorphous polymers and glass forming liquids at temperatures higher than T_g.[31,32,35] This drop in ε′(*T*) is not observed in the hybrids. This behavior resembles that of semicrystalline polymers[47] and has been observed also in other polymeric nanocomposites.[48] We think that the drop of ε′(*T*) at higher temperatures is compensated by the gradual unfreezing of molecular (segmental) motions in the hybrids, i.e. the fraction of immobilized chains at the interfaces with POSS decreases with increasing temperature. It is interesting to note in this connection that DRS measurements in poly (dimethylsiloxane)/silica nanocomposites with a fine dispersion of silica nanoparticles revealed the existence of two segmental α relaxations and showed that, with increasing temperature, the relaxation strength of the faster one, associated with the bulk polymer, increases at the expenses of the relaxation strength of the slower relaxation, associated with the bound polymer.[49] In principle, loosening of the POSS percolating network could also cause such effects. However, the results of DMA measurements on the same samples suggest that such loosening and disordering of the POSS crystalline domains

occurs at higher temperatures, see next paragraph.[25] Thus, the results in Figure 4 provide further support for the two-phase model of polymer dynamics in the hybrids postulated on the basis of the TSDC results.

The increase of $\varepsilon'(T)$ in Figure 4 at temperatures higher than about 80°C, more clearly observed for sample d_1, may be correlated with a drop of the mechanical modulus observed for the same samples in DMA measurements in the same temperature range.[25] This drop has been attributed to disordering of POSS crystalline domains in the networks, which form physical cross-links, thus increasing effective cross-linking density and rubbery modulus. It would be interesting in future to further follow this point by extending the temperature range of measurements to temperatures higher than 150°C and by analyzing the $\varepsilon'(f)$ and $\varepsilon'(T)$ dependencies at higher temperatures.

In the glassy state, at temperatures lower than about −50°C, $\varepsilon'(T)$ in Figure 4 increases in the hybrid d_1, as compared with the pure epoxy network, and decreases slightly in the hybrid d_2 with the higher POSS content. This, at first glance peculiar behavior, may be explained as follows. In the temperature range below −50°C there is no contribution of any dipolar relaxation to ε' at the high frequency of measurements of 680 kHz and ε' is determined by electronic and atomic polarization. On addition of the POSS units, ε' changes due to contribution of both the Si—O skeleton and the R groups and due to the increase in free volume, i.e. the decrease in density arising from the loosened packing of the chains. Obviously, the increase of ε' due to the addition of POSS ($\varepsilon' = 3.8$–4.0 for silica[50]) dominates over the decrease due to decrease of density in d_1, whereas the opposite is the case in d_2.

The results reported above for $\varepsilon'(T)$ are interesting with respect to the search for materials with low values of dielectric permittivity (low-κ materials) for applications as interlayer and intermetal dielectrics in microelectronics.[50] Hybrid polymer-POSS networks, in particular polyimide-POSS, have recently attracted much interest for such applications.[23] The reduction of ε' in these materials is usually attributed to increase of free volume and of porosity, as often proved by density measurements.[22,23] Often ε' is measured at a single high frequency (typically 1 MHz) and room temperature. However, in addition to low values of dielectric permittivity, also a reduced frequency and temperature dependence of ε' is required for microelectronics applications, which must be checked by measurements over wide temperature and frequency ranges similar to those reported here. Although the POSS-modified epoxy networks under investigation here are not suitable as low-κ materials, because of their low T_g values, the results in Figure 4 show that a behavior more similar to that of sample d_2, rather than that of sample d_1, is required. The demand for weak $\varepsilon'(T)$ and $\varepsilon'(f)$ dependencies, in addition to low absolute values, indicates that special attention must be paid to the investigation of the effects of the rigid inclusions on the dielectric strength of the secondary relaxations, which may contribute to $\varepsilon'(T)$ and $\varepsilon'(f)$.[29]

For the isochronal semi-log $\varepsilon''(T)$ plots in Figure 5 a low frequency of 10 Hz has been chosen in order to follow, in a single plot, all the relaxations present in the pure epoxy network and the hybrids: the local, secondary γ and β relaxations in the glassy state, the segmental α relaxation and the global NM relaxation in the temperature region of the glass transition, and dc conductivity and conductivity effects at higher temperatures. We will not further analyse dc conductivity here, we would like just to add one comment. Conductivity in Figure 5 decreases systematically in the hybrids, as compared to the pure epoxy network. This result is in agreement with and provides further support for the two-phase model of polymer dynamics in the hybrids: the number of conductive paths is reduced in the hybrids, as a result of the immobilization of a fraction of the polymer matrix.

Please note that ε'' in Figure 5 has been normalized to the same polymer fraction, $\varepsilon''_{\text{norm}} = \varepsilon''/(1 - w)$, where w is the weight fraction of the POSS units, so that the magnitudes of the relaxations (heights of the loss peaks) in the various samples can be directly compared with each other. The most striking result in Figure 5 is the significant reduction of the normalized response in the region of the glass transition in the hybrids, as compared with the pure epoxy network, in agreement with the TSDC results of Figure 2 and Table II. We will quantify these results later by fitting appropriate model functions to the isothermal $\varepsilon(f)$ data. However, before we proceed with the analysis, we would like to extract more information on the time scale and the magnitude of the four relaxations present in the networks solely on the basis of the raw data.

Figures 6 and 7 show comparative $\varepsilon''(f)$ plots of the three samples under investigation and for Jeffamine at 80°C, to follow the secondary γ and β relaxations, and at −20°C (−55°C for Jeffamine), to follow the segmental relaxation and the NM relaxation, respectively. We observe in Figure 6 for the networks that the frequency position (time scale) of the β relaxation does not practically change with composition, whereas for the γ relaxation a shift to higher frequencies is observed in the hybrids.

The secondary γ and β relaxations are present also in the pure epoxy network, so that the molecular groups responsible for these relaxations may reside either in Jeffamine or in DGEBA. Comparison with pure Jeffamine data in Figure 6 and in the Arrhenius

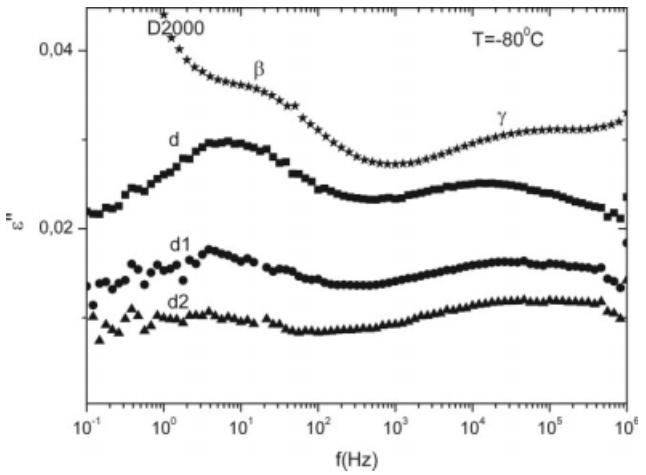

Figure 6 Comparative $\varepsilon''(f)$ plot of the three networks (with composition listed in Table I) and of Jeffamine D2000 at −80°C.

plot to be discussed later suggests that Jeffamine is the origin of both secondary relaxations. It is very likely that DGEBA itself makes a contribution to the dielectric response in the region of the secondary relaxations, which may be ignored, however, at a first stage against that of Jeffamine, as indicated by comparison with the results of dielectric measurements in epoxy resins based on DGEBA cured with low molar mass cross-linkers.[41,51,52] Please note that the two relaxations have practically the same time scale in Jeffamine and in the networks, this result providing support for the local character of the two relaxations against a relaxation of Goldstein-Johari type.[51] In agreement with previous work, the γ relaxation is assigned to local motions of $(CH_2)_n$ sequences and the β relaxation to motion of polar ether groups with attached water molecules, as confirmed also by measurements on cross-linked polyurethanes based on polymer polyols synthesized from poly(oxypropylene glycol), at various levels of humidity/water content.[53]

We turn now our attention to the α and NM relaxations shown in Figure 7. The double peak shifts slightly to higher frequencies with increasing POSS content in the hybrids, indicating an acceleration of the response in the region of the glass transition. The magnitude of the response decreases significantly in the hybrids, as shown also by the normalized $\varepsilon''(T)$ plots in Figure 5. A striking result in Figure 7, by comparing with pure Jeffamine and with data on poly(oxypropylene glycol) recorded in the region of the glass transition,[45] is the relatively very strong contribution of the NM relaxation to the double peak in the networks, which becomes evident also in Figure 5. This becomes clear also from normalized $\varepsilon''/\varepsilon''_{max}$ against f/f_{max} plots (not shown here), where ε''_{max} and f_{max} refer to the α peak. We will come back to the significance of this result in terms of morphology later after analyzing the DRS data.

Analysis of DRS data

The dielectric data, similar to those shown in Figures 3, 6, and 7, were further analyzed by fitting appropriate model functions to the measured spectra. On the basis of the previous experience,[31,32,44] a sum of two Havriliak-Negami (HN) expressions of the type[54]

$$\varepsilon^*(\omega) = \varepsilon_\infty + \frac{\Delta\varepsilon}{(1 + (i\omega\tau_{HN})^{1-\alpha})^{\beta}} \quad (2)$$

was fitted, at each temperature, to the dielectric spectra in the region of the double α-NM peak. In this expression $\varepsilon^* = \varepsilon' - i\varepsilon''$ is the complex dielectric permittivity (function), $\omega = 2\pi f$, $\Delta\varepsilon$ the intensity (magnitude, strength) of the relaxation process, $\tau_{HN} = \frac{1}{(2\pi f_{HN})}$ and f_{HN} the position of the relaxation process on the frequency scale, ε_∞ is $\varepsilon'(f)$ for $f \gg f_{HN}$ and α and β are shape parameters. For each of the two relaxations, α and NM, the frequency of maximum loss (peak frequency) f_{max} was calculated by[55]

$$f_{max} = f_{HN}\left[\frac{\sin\left[\frac{(1-a)\pi}{2+2\beta}\right]}{\sin\left[\frac{(1-a)\beta\pi}{2+2\beta}\right]}\right]^{\frac{1}{1-\alpha}} \quad (3)$$

Secondary relaxations are known to be symmetric in shape. Thus, the symmetric Cole–Cole equation, which is the HN expression with $\beta = 1$, was fitted, at each temperature to the dielectric spectra for the γ and the β relaxation. In that case $f_{max} = f_{HN}$.

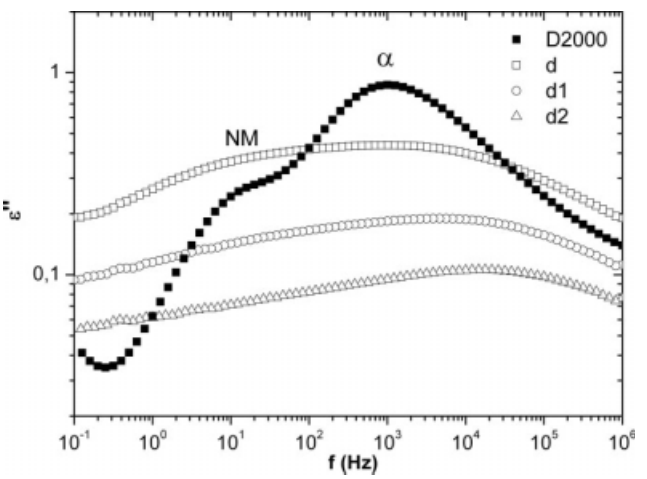

Figure 7 Comparative $\varepsilon''(f)$ plot of the networks at −20°C and of Jeffamine D2000 at −55°C.

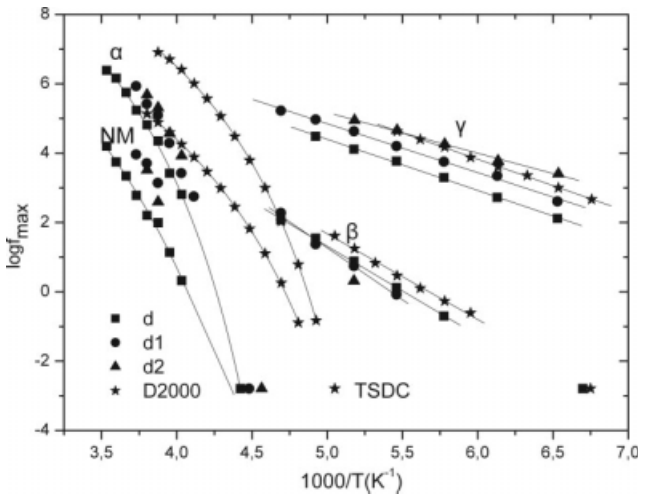

Figure 8 Arrhenius plot for the four relaxations in Jeffamine D2000 and the three networks indicated on the plot (with composition listed in Table I). Included in the plot are also TSDC data. The lines are fits of the Arrhenius eq. (4) to the γ and β data and of the VTF eq. (5) to the α and NM data.

By the fitting procedure described above, information extracted from each relaxation is quantified in terms of time scale (f_{max}), magnitude (Δε) and shape (α, β) of the response. In the following, we focus on the information on time scale and magnitude of the four relaxations present in the materials under investigation.

Time scale is best discussed in terms of the Arrhenius plot (activation diagram) shown in Figure 8 for the four relaxations (γ, β, α, NM) and the three networks studied, as well as pure Jeffamine D2000 for comparison. Included in the plot are also TSDC data (Fig. 2) at the equivalent frequency of 1.6×10^{-3} Hz, corresponding to a relaxation time of 100s.[44,53] We observe in Figure 8 that the γ relaxation becomes clearly slower in the pure epoxy network (sample d), as compared to Jeffamine. With respect to the pure epoxy network, the relaxation becomes faster with increasing POSS content in the hybrids. Similar to the γ relaxation, the β relaxation becomes slower in the pure network, as compared to pure Jeffamine. Results are less clear with respect to the effects of POSS on the β relaxation, since less data on two samples only could be analyzed.

Both cooperative relaxations in Figure 8, the segmental α relaxation and the normal mode relaxation, become significantly slower in the networks, as compared to pure Jeffamine. Regarding the effects of POSS nanoparticles, the segmental α relaxation becomes faster with increasing POSS content in the hybrids, in excellent agreement with the TSDC data. Also the NM relaxation becomes faster in the hybrids. We observe in Figure 8 that α and NM approach each other with decreasing temperature toward T_g, as expected for oligomers[44,45] and is clearly observed for Jeffamine and the pure epoxy network, i.e. the network with the larger response. Please note that this closer merging of the two relaxations, combined with the reduction of the response in the hybrids (Fig. 7), makes results of the analysis more ambiguous, in particular for the weaker NM relaxation. This approaching and merging of the α and the NM relaxations with decreasing temperature, as the cooperativity length (characteristic length) of the glass transition[35] increases toward the chain length of Jeffamine, makes also clear now why two relaxations are clearly observed in the DRS spectra, at least at high temperatures (high frequencies), whereas only one in the TSDC spectra. Because of the larger contribution of α to the double α-NM peak it is also reasonable that we treated the TSDC peak in terms of the α relaxation.

It is interesting to note the very good agreement of the TSDC and the DRS data in Figure 8, not only with respect to the trends observed, e. g. the acceleration of the α relaxation in the hybrids, but also with respect to absolute values of f_{max}. This coincidence, observed also in previous work,[34,53] is an important fact from the methodological and the metrological point of view, as it allows to practically extend the frequency range of dielectric measurements down to low frequencies not easily accessible by DRS.

The data for the temperature dependence of the time scale of the dielectric response were further analyzed by fitting appropriate functions to the $f_{max}(T)$ data for each relaxation. The Arrhenius equation[35,49]

$$f_{max} = f_o \exp\left(-\frac{W}{kT}\right) \quad (4)$$

where W the activation energy (barrier height), k Boltzmann's constant, and f_0 a frequency factor, was fitted to the data for the secondary γ and β relaxations and the fitting parameters are listed in Table III. They are in the range of values reported previously for the γ and β relaxations in polyurethanes based on poly(oxypropylene glycol),[53] thus providing further support for the assignment of the relaxations at the molecular level. Similar values of the activation parameters are obtained in pure Jeffamine

TABLE III
Fitting Parameters W and f_0 of the Arrhenius Equation (4) for the γ and β Relaxations in Figure 8

	β relaxation		γ relaxation	
Sample	f_o (Hz)	W (kJ/mol)	f_o (Hz)	W (kJ/mol)
D2000	1×10^{14}	48	1×10^{13}	29
d	2×10^{14}	51	1×10^{12}	30
d1	2×10^{16}	59	8×10^{11}	28
d2	–	–	1×10^{11}	23

and in the networks, providing further support that both secondary relaxations originate from Jeffamine.

The Vogel-Tammann-Fulcher (VTF) equation[35,49]

$$f_{\max} = A \exp\left(-\frac{B}{T - T_0}\right) \quad (5)$$

characteristic of cooperative processes, where A, B, and T_0 (Vogel temperature) are temperature independent empirical constants, was fitted to the data for the α and the NM relaxations, only for Jeffamine and the pure epoxy network, where more data were available, with reasonable values of the fitting parameters ($\log A = 12.2$, $B = 1080$ K, $T_0 = 162$ K for α and $\log A = 10.1$, $B = 1166$ K, $T_0 = 157$ K for the NM relaxation in Jeffamine; $\log A = 11.8$, $B = 1071$ K, $T_0 = 196.7$ K for α and $\log A = 12.4$, $B = 2115$ K, $T_0 = 171$ K for the NM relaxation in the pure epoxy network).

Thus, the results of broadband DRS and of TSDC show clearly that the segmental α relaxation and the NM relaxation become slightly but systematically faster in the hybrids with increasing POSS content, as compared to the pure epoxy network. The corresponding reduction of T_g, from the TSDC data, is 3 and 7°C for the samples with 35 and 50 wt % POSS units, respectively, as compared with the pure epoxy network (Table II). The secondary γ relaxation becomes also systematically faster in the hybrids (increase of $f_{\max}$ by more than one decade in Fig. 8) with a corresponding decrease of the activation energy (Table III). On the other hand, the time scale of the secondary β relaxation seems not to be affected, however results are less clear for this relaxation. Please note also that normalized plots of $\varepsilon''/\varepsilon''_{\max}$ against $f/f_{\max}$ show a broadening of the response of the γ relaxation in the hybrids. A possible explanation for the different behavior of the secondary β and γ relaxations in the hybrids with respect to time scale of the response is that the γ relaxation, arising from crankshaft motion of methylene sequences, refers to a larger unit, i. e. it is more affected by changes induced by the presence and bonding of the bulky POSS units, as compared to the β relaxation, which arises from motion of the smaller ether groups. The acceleration of the α, NM, and γ relaxations in the hybrids can be explained in terms of increase of free volume, arising from loosened molecular packing of the chains due to the presence of the rigid and bulky POSS units and their covalent bonding to the chains, as confirmed by the results of density measurements reported in a previous section. Plasticization by the bulky POSS units[3] is a different terminology for the same effect. DRS measurements in poly(bisphenol A carbonate) (PBAC)-POSS nanocomposites prepared by solution blending, have shown that both the segmental α relaxation and the secondary β relaxation of PBAC become faster with increasing POSS content.[36] The results have been explained in terms of plasticization of PBAC due to a decrease of the packing density, which is rationalized by density measurements. As pointed out by the authors, the plasticization by the PBAC matrix is different from that caused by conventional low-molecular weight plasticizers, where, in general, α becomes faster and β slower with respect to the pure polymer.[36]

Unlike the segmental α relaxation and the glass transition, there are only a few reports in the literature on the effects of nanoparticles on the NM relaxation in polymer nanocomposites. Page and Adachi[46] employed DRS to investigate the behavior of the segmental α relaxation and the NM relaxation in blends of sodium montmorillonite particles and a series of low-molecular weight polymers (polyisoprene, poly(propylene glycol), poly(butylenes oxide)), which are known to exhibit the NM relaxation. Next to an α and a NM relaxation with properties similar to those of the bulk polymer, assigned to the polymer outside the galleries, a faster α relaxation was observed and assigned to intercalated polymer. The NM of the intercalated polymer was not observed, since it occurs at higher temperatures and lower frequencies, where the dielectric loss due to dc conduction overwhelms the signal of the dipolar relaxation.[46] Mijovic et al.,[56] on the other hand, employed DRS and dynamic mechanical spectroscopy to investigate effects of the type and concentration of the clay and of the molecular weight of the polymer on polymer dynamics in nanocomposites of organically modified clay nanoparticles and polyisoprene. For low-molecular-weight polyisoprene no effect of clay loading on the average relaxation time for segmental and NM relaxation was observed. For high-molecular-weight polyisoprene (in the entangled regime), however, an acceleration of the NM relaxation was observed, explained by preferential suppression of the longer scale portion of the NM spectrum.[56]

The relaxation strength of each of the four relaxation processes, obtained from the fitting of the HN expression (2) to the experimental data, was normalized to the same mass fraction of the polymer, $\Delta\varepsilon_n = \Delta\varepsilon/(1 - w)$, where w the mass fraction of the POSS units. Please note that the normalisation remains valid, regardless of the origin of each of the relaxation processes (from Jeffamine or DGEBA), as the ratio of functional groups r = NH/epoxy was kept constant, equal to 1, throughout this work. $\Delta\varepsilon_n$ was plotted as a function of temperature for each of the processes. The plots, not shown here, reveal, as expected from the literature,[31,32] an increase of $\Delta\varepsilon_n$ with increasing temperature for the secondary relaxations and a decrease for the segmental α relaxation.

TABLE IV
Relaxation Strength $\Delta\varepsilon_n$ of the Various Processes, Normalized to the Mass Fraction of the Polymer, Mean Values Over the Temperature Range of Measurements (details in text)

Sample	γ relaxation	β relaxation	α relaxation	NM relaxation
D2000	0.30	0.20	3.20	0.50
d	0.30	0.21	2.35	1.83
d1	0.29	0.29	1.53	1.70
d2	0.27	–	1.09	0.75

What is unexpected is the observed clear increase of $\Delta\varepsilon_n$ with increasing temperature for the NM relaxation, as it is well established that for homopolymers $\Delta\varepsilon_n$ decreases with increasing temperature, even faster than $\Delta\varepsilon_n$ for the segmental α relaxation.[44,45] This increase may be related with the structure ordering found in DGEBA-Jeffamine networks[57] and a disordering at higher temperatures.

Table IV lists mean values of $\Delta\varepsilon_n$, over the temperature range of measurements, for the four relaxation processes. The temperature range of measurements is approximately from −140 to −70°C and from −100 to −60°C for the γ and β relaxation, respectively, for all samples. For the α and the NM relaxation this range is approximately from −65 to −45°C for the Jeffamine and from −30 to −5°C for the three networks. Similar to the results of analysis for the time scale of the relaxations summarized in the Arrhenius plot of Figure 8 and in Table III, the results listed in Table IV quantify observations made already on the basis of the raw data in the comparative plots of Figures 4–7. Bearing in mind some ambiguity in the determination of the fitting parameters and of mean values over the temperature range of measurements (and in agreement with conclusions based on the raw data of Figures 4–7), $\Delta\varepsilon_n$ of the secondary γ and β relaxations does not show any significant variation with composition of the networks. Moreover, similar values of $\Delta\varepsilon_n$ have been obtained in pure Jeffamine and in the networks. The most striking result in Table IV is the significant reduction of $\Delta\varepsilon_n$ of the segmental α relaxation and of the NM relaxation in the hybrids. These results suggest that the normalized magnitude of the local relaxations is not affected by the presence of the POSS units and the resulting morphology investigated in reference.[9] On the contrary, the normalized magnitude of the more extended cooperative processes, α and NM, is significantly reduced in the hybrids, as compared to the pure network. A possible explanation for this behavior, consistent with the results on time scale of the relaxations (Fig. 8), is that a significant part of the chains is immobilized due to the presence of and interactions with the rigid POSS units. This immobilization refers to the cooperative α and NM relaxations, however not to the local, secondary γ and β relaxations.

The normal mode relaxation in Figure 7 and in Table IV exhibits, relatively to the α relaxation and also absolutely, high values of relaxation strength in the networks, as compared to pure Jeffamine and to results obtained with poly(oxypropylene glycol) homopolymers.[45] Interestingly, Mijovic and coworkers[56] observed an increase of the dielectric strength of the NM relaxation with clay content in polyisoprene/clay nanocomposites, regardless of the type of clay and the molecular weight of the polymer, which was explained in terms of a conformational change and an increase in the end-to-end distance of intercalated polymer chains. It is well-known from the theory that the relaxation strength of the NM relaxation increases with the square of chain length (end-to-end polarization vector o the chain).[43] Measurements in poly(oxybutylene) (B) oligomers of various molar masses and in block copolymers of poly(oxybutylene) and poly(oxyethylene) (E), EB, and EBE, where the E blocks are crystalline and the B blocks amorphous, have shown that, at each molar mass of the B block, the normalized relaxation strength of the NM relaxation of the B blocks increases significantly in the diblocks and even more in the triblocks, as compared to the homopolymers.[44] These results have been explained in terms of extension of the B blocks in the block copolymers. Thus, the results in Figure 7 and in Table IV suggest that Jeffamine, the origin of the NM relaxation in our epoxy networks, is stretched in the networks, in agreement with and in support of a structure model of the networks proposed on the basis of SAXS, WAXS and TEM measurements.[9]

CONCLUSIONS

Molecular dynamics in epoxy networks, prepared from DGEBA and poly(oxypropylene)diamine (Jeffamine D2000) and modified with covalently bound dangling POSS units, was investigated in detail by calorimetry (DSC) and, mainly, by dielectric techniques (broadband DRS and TSDC, a special dielectric technique in the temperature domain). For comparison, pure Jeffamine D2000 was also investigated. The POSS- modified networks were prepared and investigated with respect to structure/morphology and thermomechanical properties by Matejka and coworkers.[9,25] Four dielectric relaxations were observed and analyzed in detail, the local, secondary γ and β relaxations in the glassy state and the segmental α and the normal mode (NM) relaxations in the temperature region of the glass transition. The latter arises from the fluctuation and orientation of the end-to-end polarization vector of the chain in the

electric field, related with the presence of a dipole moment component along the Jeffamine chain contour. Thus, dielectric techniques are particularly suited for dynamics studies in the epoxy networks based on Jeffamine. The normal mode relaxation makes a relatively strong contribution to the spectra, providing support for an extended conformation of Jeffamine in the networks.

The results, by both DSC and the dielectric techniques, show a significant increase of heterogeneity of dynamics in the region of the glass transition, which reflects a spatial heterogeneity. The results by both dielectric techniques, normalized to the same polymer fraction in the networks, show a significant reduction of the dielectric response in the region of the glass transition (cooperative α and NM relaxations) and practically no changes in the magnitude of the local, secondary relaxations. At the same time, the dynamics of the α and the NM relaxations, and of the secondary γ relaxation as well, becomes slightly but systematically faster in the hybrids, as compared with the pure network. It is interesting to note that analysis of DMA loss modulus data in terms of glass transition reveals similar trends.

These results may be explained in terms of a two-phase model of polymer dynamics based on two contradictory effects of the presence of the bulky POSS units and their covalent bonding to the chains: constraints imposed to the motion of the polymer chains by the rigid particles and, at the same time, increase of free volume due to loosened molecular packing of the chains. The increase of free volume has been confirmed by density measurements. As a result, a significant portion of the chains is immobilized, probably at interfaces with POSS particles, whereas the rest exhibits a slightly faster dynamics. Immobilization refers only to long-scale motions (segmental α relaxation and normal mode relaxation), however not to local-scale motions (secondary relaxations). Various versions of a two-phase model of polymer dynamics have already been used to explain results obtained with polymer nanocomposites typically in terms of an interfacial layer with a slower dynamics and the bulk with dynamics similar or slightly modified with respect to that of the pure matrix polymer.[38,40,49,58,59] Please note that the papers cited above refer to a variety of polymer matrices (thermoplastics, thermosets, rubbers) and nanofillers (silica, clays).

Several results obtained within this work provide support for the two-phase model of polymer dynamics. In future it would be interesting to quantify this model (in terms of fraction of immobilized polymer and of interfacial layer thickness[49]) by extending measurements to several compositions, in particular with low POSS fractions, and to other POSS topologies.

References

1. Pittman, C. U.; Ni, H.; Wang, L.; Li, G. J Inoorg Organomet Polym 2001, 11, 123.
2. Phillips, S. H.; Haddad, T. S.; Tomczak, S. J. Curr Opin Solid State Mater Sci 2004, 8, 21.
3. Pielichowski, K.; Njunguna, J.; Janowski, B.; Pielichowski, J. Adv Polym Sci 2006, 201, 225.
4. Schwab, J. J.; Lichtenhan, J. D. Appl Organomet Chem 1998, 12, 707.
5. Sellinger, A.; Laine, R. M. Macromolecules 1996, 29, 2327.
6. Lu, T.; Liang, G.; Guo, Z. J Appl Polym Sci 2006, 101, 3652.
7. Liang, K.; Li, G.; Toghiani, H.; Koo, J. H.; Pittman, C. U. Chem Mater 2006, 18, 301.
8. Choi, J.; Kim, S. G.; Laine, R. M. Macromolecules 2004, 37, 99.
9. Matejka, L.; Strachota, A.; Plestil, J.; Whelan, P.; Steinhardt, M.; Slouf, M. Macromolecules 2004, 37, 9449.
10. Fu, B. X.; Gelfer, M. Y.; Hsiao, B. S.; Phillips, S.; Viers, B.; Blanski, R.; Ruth, R. Polymer 2003, 44, 1499.
11. Lichtenhan, J. D.; Haddad, T. S.; Schwab, J. J.; Carr, M. J.; Chaffee, K. P.; Mather, P. T. Polym Prepr 1998, 39, 489.
12. Zhao, Y.; Schiraldi, D. A. Polymer 2005, 46, 11640.
13. Xu, H. Y.; Kuo, S. W.; Lee, J. S.; Chang, F. C. Macromolecules 2002, 35, 8788.
14. Bharadwaj, R. K.; Berry, R. J.; Farmer, B. L. Polymer 2000, 41, 7209.
15. Toepfer, O.; Neumann, D.; Choudhury, N. R.; Whittaker, A.; Matisons, J. Chem Mater 2005, 17, 1027.
16. Kopesky, E. T.; Haddad, T. S.; Cohen, R. E.; McKinley, G. H. Macromolecules 2004, 37, 8992.
17. Fu, B. X.; Namani, M.; Lee, A. Polymer 2003, 44, 7739.
18. Dell'Erba, I. E.; Fasce, D. P. R.; Williams, R. J. J.; Erra-Balsells, R.; Fukuyama, Y.; Nonami, H. Macromol Mater Eng 2004, 289, 315.
19. Li, G. Z.; Wang, L. C.; Toghiani, H.; Daulton, T. L.; Koyama, K.; Pittman, C. U. Macromolecules 2004, 34, 8686.
20. Lee, A.; Lichtenhan, J. D. Macromolecules 1998, 31, 4970.
21. Goertzen, W. K.; Kessler, M. R. J Appl Polym Sci 2008, 109, 647.
22. Leu, C.-M.; Chang, Y.-T.; Wie, K.-H. Chem Mater 2003, 15, 3721.
23. Lee, Y.-J.; Huang, J.-M.; Kuo, S.-W.; Lu, J.-S.; Chang, F.-C. Polymer 2005, 46, 173.
24. Lee, J. H.; Lyu, Y. Y.; Lee, M. S.; Hahn, J.-H.; Rhee, J. H.; Mah, S. K.; Yim, J.-H.; Kim, S. Y. Macromol Mater Eng 2004, 289, 164.
25. Strachota, A.; Kroutilova, I.; Kovarova, J.; Matejka, L. Macromolecules 2004, 37, 9457.
26. Shan, L.; Verghese, K. N. E.; Robertson, C. G.; Reifsnider, K. L. J Polym Sci Part B Polym Phys 1999, 37, 2815.
27. Park, I.; Peng, H.; Gidley, D. W.; Xue, S.; Pinnavaia, T. J. Chem Mater 2006, 18, 650.
28. Bershtein, V. A.; Egorova, L. M.; Yakushev, P. N.; Pissis, P.; Sysel, P.; Brozova, L. J Polym Sci Part B Polym Phys 2002, 40, 1056.
29. Fragiadakis, D.; Logakis, E.; Pissis, P.; Kramarenko, V. Y.u; Shantalii, T. A.; Karpova, I. L.; Dragan, K. S.; Privalko, E. G.; Usenko, A.; Privalko, V. P. J Phys Conf Ser 2005, 10, 13942.
30. Van Turnhout, J.In Electrets: Topics in Applied Physics; Sessler, G. M., Ed.; Springer: Berlin, 1980; Vol. 33, p 81.
31. Kremer, F.; Schoenhals, A., Eds. Broadband Dielectric Spectroscopy, Springer: Berlin, 2002.
32. Runt, J. P.; Fitzgerald, J. J., Eds. Dielectric Spectroscopy of Polymeric Materials, American Chemical Society: Washington, DC, 1997.
33. Hensel, A.; Dobbertin, J.; Schawe, E. K.; Boller, A.; Schick, C. J Therm Anal 1996, 46, 935.
34. Vatalis, A. S.; Kanapitsas, A.; Delides, C. G.; Viras, K.; Pissis, P. J Appl Polym Sci 2001, 80, 1071.

35. Donth, E.The Glass Transition: Relaxation Dynamics in Liquids and Disordered Materials, Springer: Berlin, 2001.
36. Hao, N.; Boehning, M.; Goering, H.; Schoenhals, A. Macromolecules 2007, 40, 2955.
37. Dobbertin, J.; Hensel, A.; Schick, C. J Therm Anal 1996, 47, 1027.
38. Pattanayak, A.; Jana, S. C. Polymer 2005, 46, 3394.
39. Gomez Tejedor, J. A.; Rodriguez Hernandez, J. C.; Gomez Ribelles, J. L.; Monleon Pradas, M. J Macromol Sci Phys 2007, 46, 43.
40. Sargsyan, A.; Tonoyan, A.; Davtyan, S.; Schick, C. Eur Polym J 2007, 43, 3113.
41. Maggana, C.; Pissis, P. J Macromol Sci Phys 1997, 36, 749.
42. Brus, J.; Urbanova, M.; Strachota, A. Macromolecules 2008, 41, 372.
43. Watanabe, H.; Yamada, H.; Urakawa, O. Macromolecules 1995, 28, 6443.
44. Kyritsis, A.; Pissis, P.; Mai, S.-M.; Booth, C. Macromolecules 2000, 33, 4581.
45. Ngai, K. L.; Schoenhals, A.; Schlosser, E. Macromolecules 1992, 25, 4915.
46. Page, K. A.; Adachi, K. Polymer 2006, 47, 6406.
47. Neagu, E.; Pissis, P.; Apekis, L. J Appl Phys 2000, 87, 2914.
48. Kanapitsas, A.; Pissis, P.; Kotsilkova, R. J Non-Cryst Solids 2002, 305, 204.
49. Fragiadakis, D.; Pissis, P.; Bokobza, L. J Non-Cryst Solids 2006, 352, 4969.
50. Maier, G. Prog Polym Sci 2001, 26, 3.
51. Beiner, M.; Ngai, K. L. Macromolecules 2005, 38, 7033.
52. Fitz, B.; Andjelic, S.; Mijovic, J. Macromolecules 1997, 30, 5227.
53. Kanapitsas, A.; Pissis, P. Eur Polym J 2000, 36, 1241.
54. Havriliak, S. Jr.; Havriliak, S. J. Dielectric and Mechanical Relaxation in Materials, Hanser: Munich, 1997.
55. Diaz-Calleja, R. Macromolecules 2000, 33, 8924.
56. Mijovic, J.; Lee, H.; Kenny, J.; Mays, J. Macromolecules 2006, 39, 2172.
57. Beck Tan, N. C.; Bauer, B. J.; Plestil, J.; Barnes, D. J.; Liu, D.; Matejka, L.; Dusek, K.; Wu, W. L. Polymer 1999, 40, 4603.
58. Matejka, L.; Dukh, O.; Kolarik, J. Polymer 2000, 41, 1449.
59. Arrighi, V.; McEwen, I.; Qian, H.; Prieto, M. Polymer 2003, 44, 6259.